Bioorganic & Medicinal Chemistry Letters 20 (2010) 6331–6358

Contents lists available at ScienceDirect

Bioorganic & Medicinal Chemistry Letters

journal homepage: www.elsevier.com/locate/bmcl

Bioorganic & Medicinal Chemistry Letters Volume 20, Issue 22, 2010

Contents

REGULAR ARTICLES

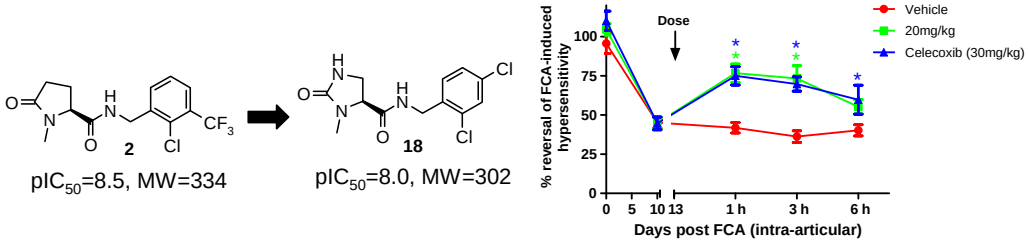

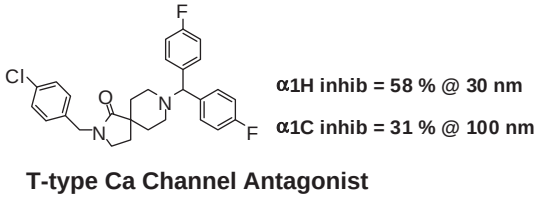

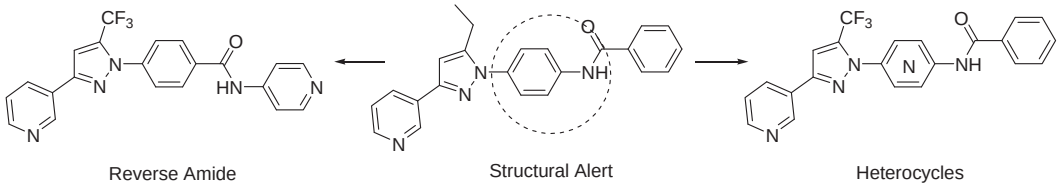

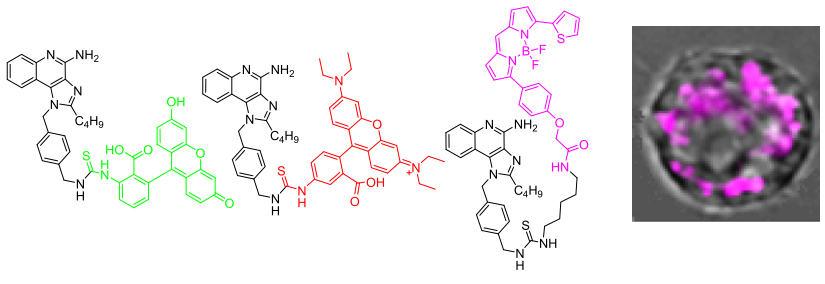

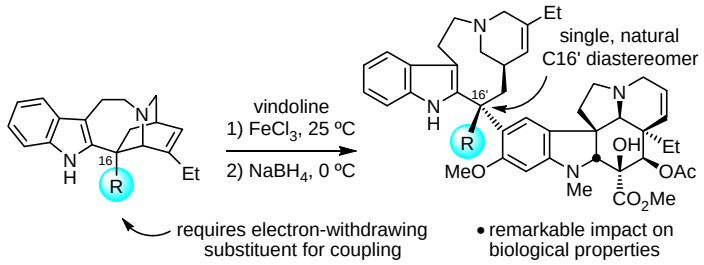

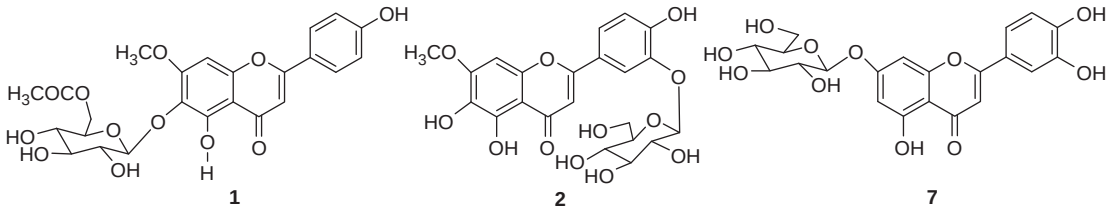

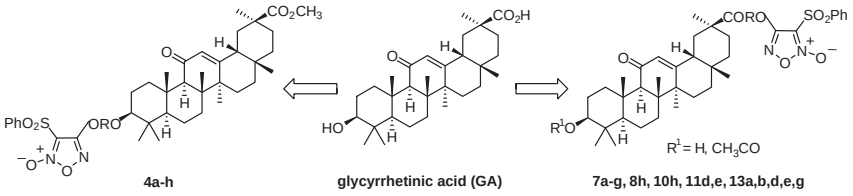

A series of novel furoxan-based nitric oxide (NO)-releasing derivatives of glycyrrhetinic acid were synthesized and evaluated for their cytotoxicity against human hepatocellular carcinoma (HCC) cells and NO-releasing ability. Five hybrids displayed selective cytotoxicity against HCC cells with a little effect on the growth of LO2 cells.

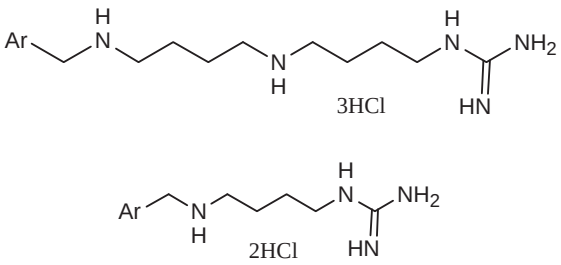

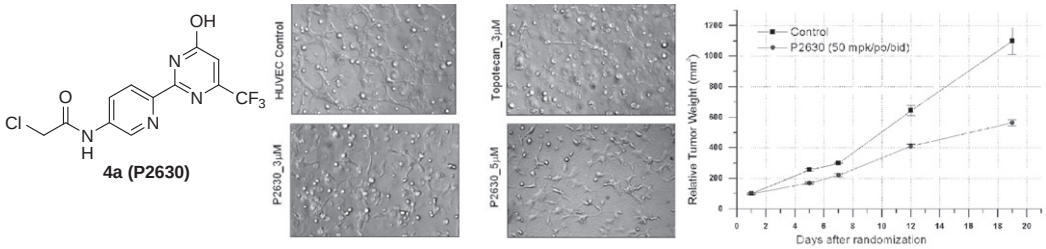

Systemic application of compound P2630, a novel HIF-1α inhibitor, significantly suppresses the cell proliferation angiogenesis. P2630 has been shown orally efficacious in PC-3 xenograft mice model.

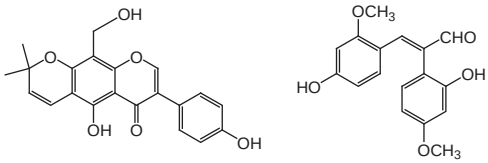

1 **2**

Two new compounds (**1** and **2**) along with seven known flavonoid derivatives (**3**–**9**) were isolated as active principles from an EtOAc-soluble extract of the root bark of *Erythrina addisoniae*. All the isolated compounds (**1**–**9**) were tested for their inhibitory activities against both influenza neuraminidases from influenza H1N1 and H9N2. Compound **2**, which is a formylated stilbenoid derivative, exhibited strong inhibition of both influenza H1N1 and H9N2 neuraminidases with IC_{50} values of 8.80 ± 0.34 μg/mL and 7.19 ± 0.40 μg/mL, respectively.

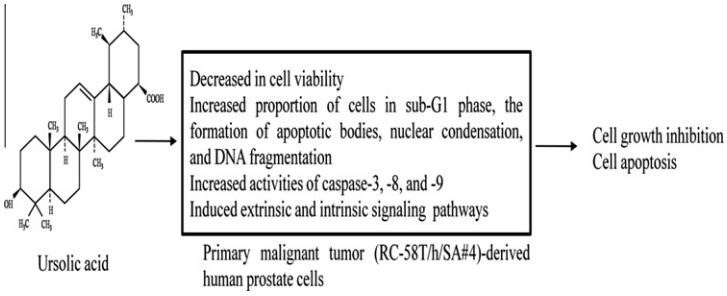

Ursolic acid from Corni fructus activated apoptosis in RC-58T/h/SA#4 cells via both caspase-dependent and -independent pathways.

Arylpiperazine-containing pyrimidine 4-carboxamide derivatives were synthesized and evaluated as novel anti-depressant compounds. The various analogues were prepared and bio-assayed for binding to 5-HT_{2A}, $5HT_{2C}$ receptor, serotonin transporter. Based on the outcomes of in vitro SAR studies, forced swimming test along with locomotor activities, **16d** was identified as a lead compound.

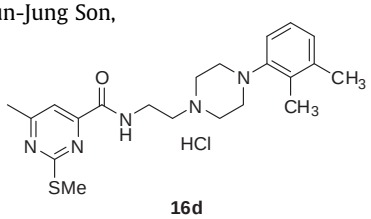

16d

5-HT_{2A} = 47 nM
5-HT_{2C} = 148 nM
SERT = 1014 nM

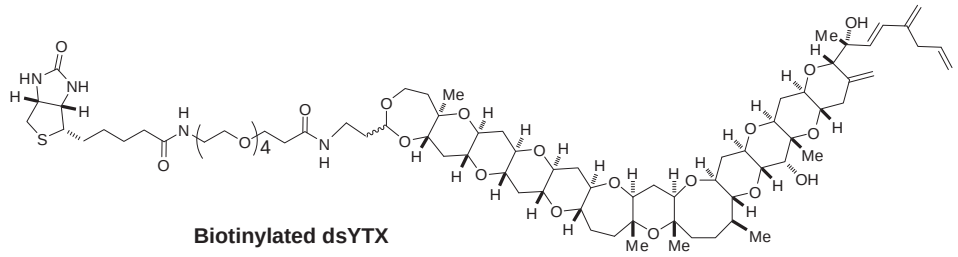

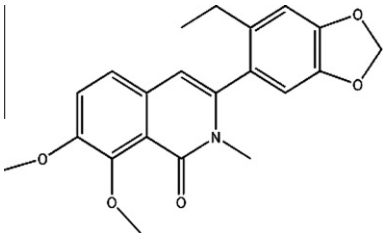

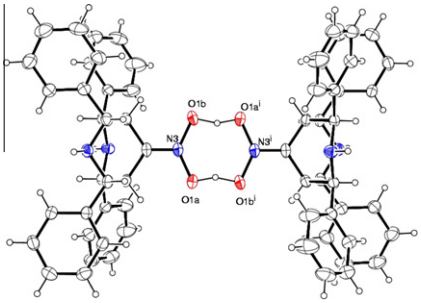

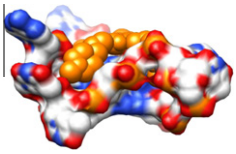

Modelled structure of a naphthalene diimide derivative with four *N*-methylpiperazine end-groups, bound to a parallel form of the human intramolecular telomeric G-quadruplex.

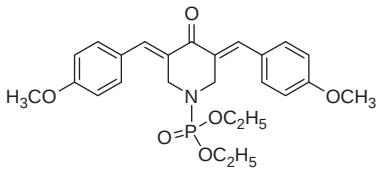

Diethyl ((3*E*,5*E*)-3,5-bis(4-methoxybenzylidene)-4-oxopiperidin-1-yl)phosphonate emerged as a lead potent cytotoxin displaying greater toxicity for neoplasms than normal cells and possesses pleiotropic and suitable druglike properties.

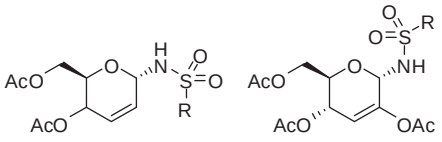

A series of α-D-hex-2-enopyranosyl sulfonamides was evaluated for their antiproliferative activity against human hepatocellular liver carcinoma (HepG2) and human lung adenocarcinoma (A549) cell lines.

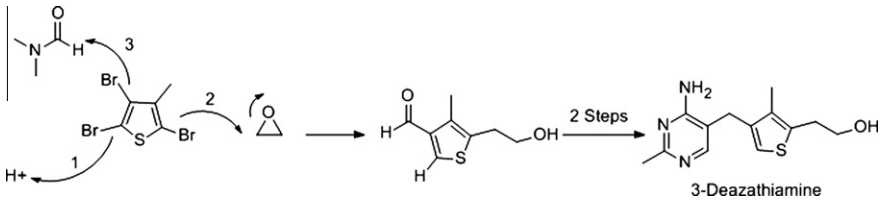

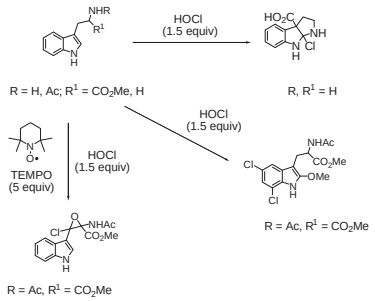

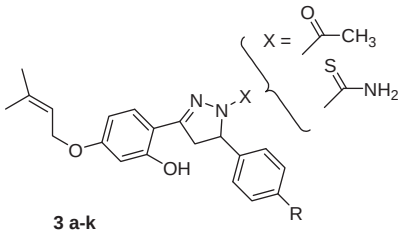

New prenylated pyrazolines were synthesized and tested on human monoamine oxidase-A and -B isoforms.

Structure-guided techniques were used to evolve a 5-pyridinyl pyrazole-3-carboxylate fragment into a series of 5-aryl-carbamoyl-3-phenyl-imidazole-4-carboxylates, examples of which inhibited the Pin1 PPIase with sub-μM IC_{50} and blocked proliferation of prostate cancer cells.

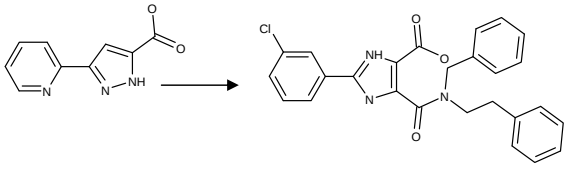

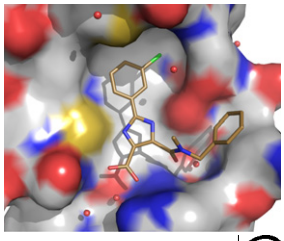

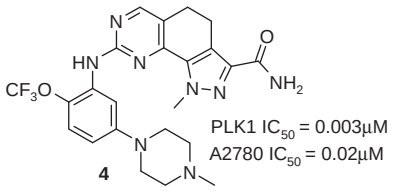

A 4,5-dihydro-1*H*-pyrazolo[4,3-*h*]quinazoline series of Polo-like kinase inhibitors is reported and the SAR disclosed. The series led to low nanomolar PLK1 inhibitors. Compound **4** was tested in vivo showing good antitumor efficacy after iv administration.

A series of N-substituted acetamidines and 2-methylimidazole derivatives structurally related to W1400 were synthesized and evaluated as Nitric Oxide Synthase (NOS) inhibitors. A molecular modeling study allowed to shed light on the effects of the structural modifications on the selectivity of the designed inhibitors toward the different NOS isoforms.

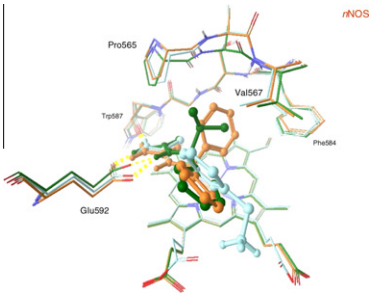

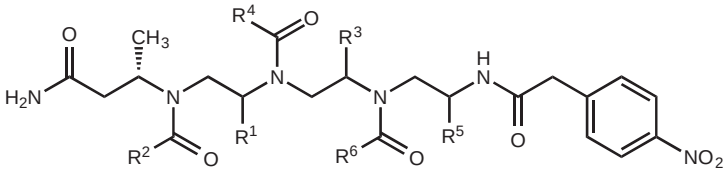

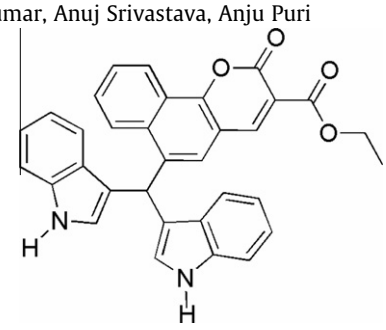

The discovery of new series of coumarin bisindoles as potential antidyslipidemic agents is described.

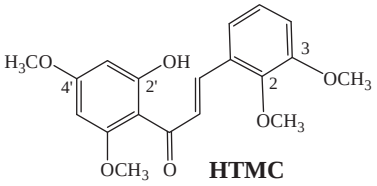

Chalcone derivative 2′-hydroxy-2,3,4′,6′-tetramethoxychalcone (HTMC) inhibited the growth of human lung cancer cell lines without cytotoxic to normal cells. In A549 lung adenocarcinoma cells, HTMC caused G1 phase cell-cycle arrest, inhibited the cell-cycle regulatory proteins phosphorylation of cdc2 (Tyr^{15} and Tyr^{161}) and Rb (Ser^{795} and $Ser^{807/811}$), and accumulated the tumor suppresser genes p53 and p21. In addition, in vivo data demonstrated that HTMC act as a tumor growth suppressing agent.

A multifunctional diaminobutane poly(propylene imine) dendrimer bearing a protective PEG-coating and a folate targeting ligand is prepared, which efficiently encapsulates anticancer drug etoposide. This polymer, due to its low toxicity and cell specificity, can be applied as a targeted drug delivery system.

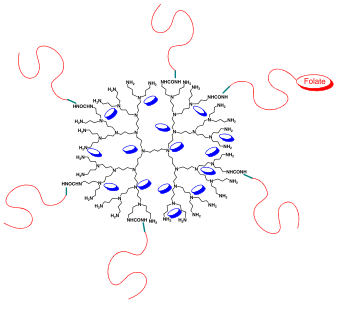

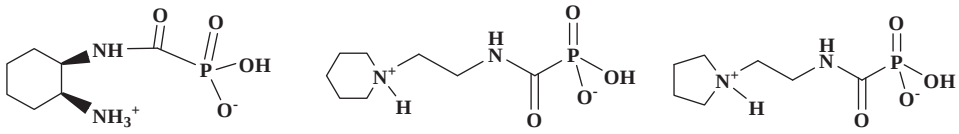

cis-ACCP PIP-CPO PYR-CPO

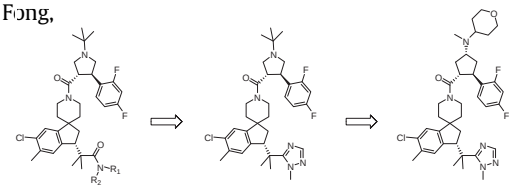

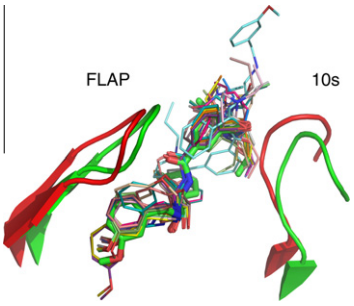

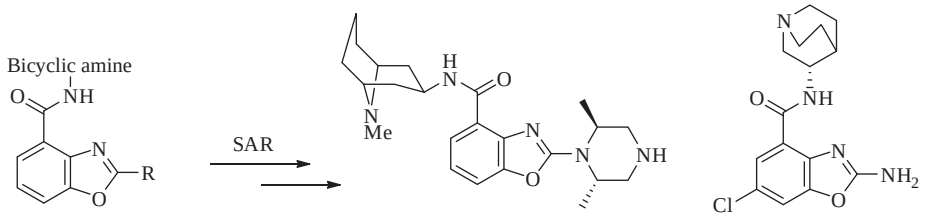

R = aryl, alkyl or amino **41**: 5-HT$_{3A}$ K_i = 2.4 nM **48**: 5-HT$_{3A}$ K_i = 4.7 nM

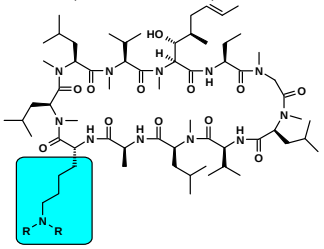

39 R = Me
43 R = Et

An efficient synthesis of [D-lysine]^{8}cyclosporin A has been developed. Several analogs of [D-lysine]^{8}cyclosporin A have been synthesized and show promising anti-HCV activity, particularly compounds **39** and **43**, which each exhibit an anti-HCV EC_{50} <200 nM, and are each ⩾50-fold less immunosuppressive than cyclosporin A.

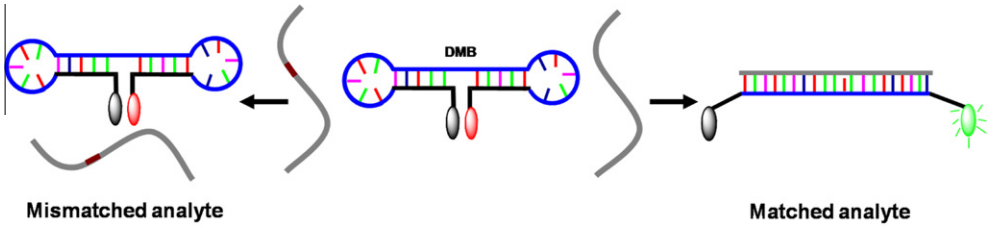

A fluorescent probe with a dumbell structure for the specific detection of target analyte and mismatched ones.

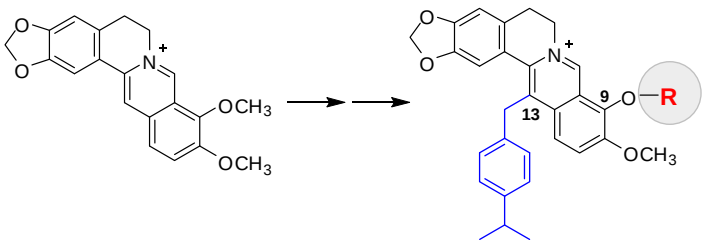

A novel series of 9-O-substituted-13-(4-isopropylbenzyl)berberine derivatives as antifungal agents was synthesized and examined the activity.

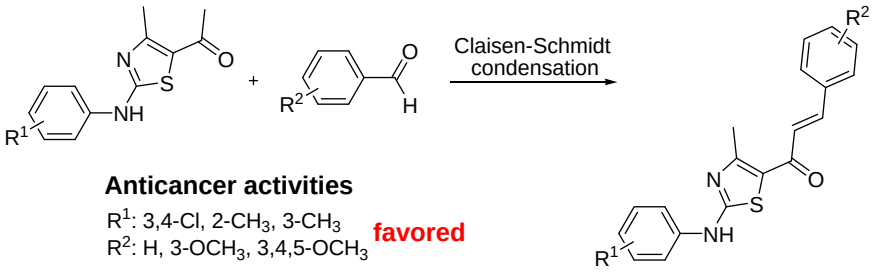

Thiazolyl–chalcones were synthesized via Claisen-Schmidt condensation and their in vitro and in vivo anticancer activities were evaluated.

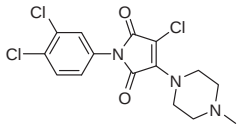

"Hit" **1**

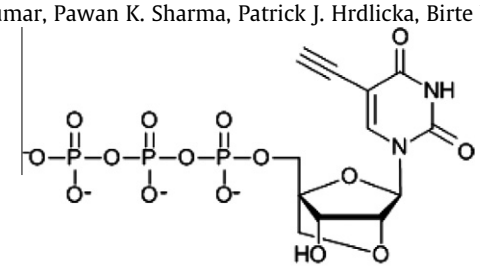

C5-ethynyl LNA-UTP

C5-Ethynyl LNA-U nucleoside 5′-triphosphate has been synthesized and investigated the enzymatic recognition capabilities. Phusion and KOD DNA polymerases were found to be efficient to incorporate C5-ethynyl LNA-U nucleotides and afforded full-length extension products.

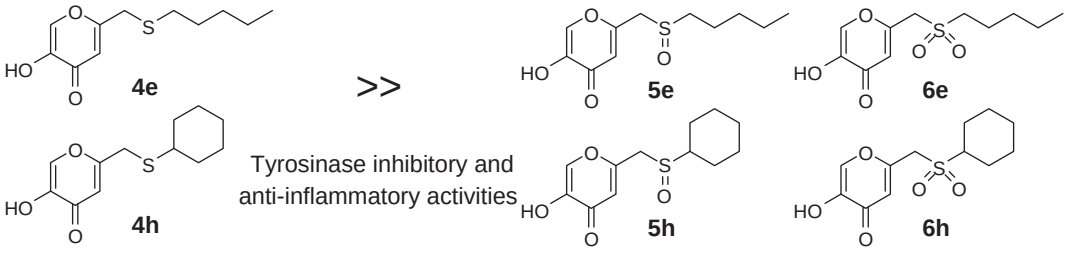

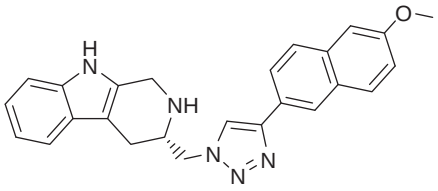

JJCA-140

A focused library from 22 different alkynes and an azide-containing tryptoline pharmacophore from virtual screening were synthesized by Cu(I)-catalyzed [3+2] azide-alkyne cycloaddition reaction. The lead compound (JJCA-140) showed IC_{50} of 1.49 μM against BACE1 and 100 times more selective to BACE1 than Cathepsin-D.

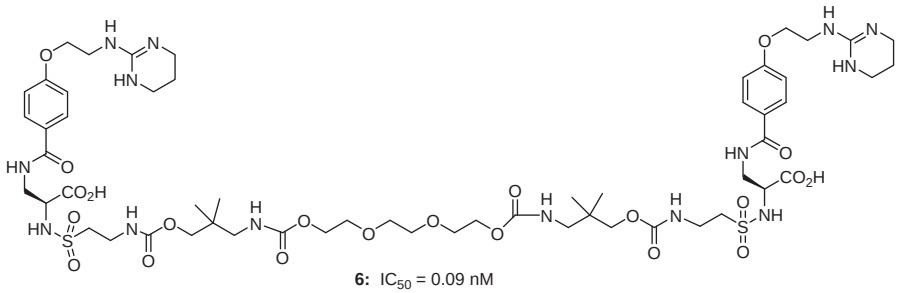

6: IC_{50} = 0.09 nM

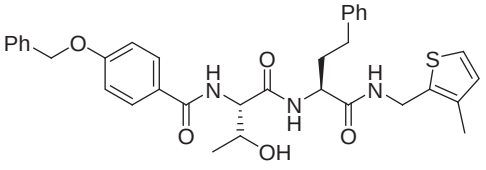

25

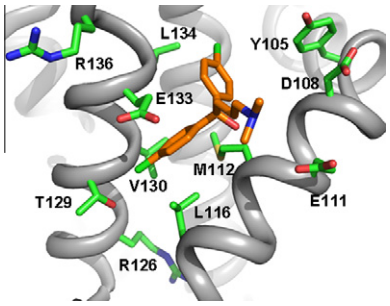

1 **14**

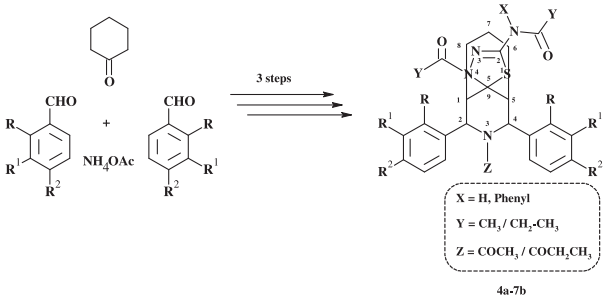

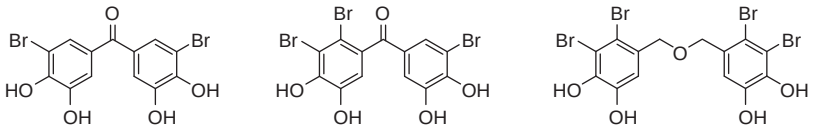

The synthesis and bioactivity of bromophenols are described.

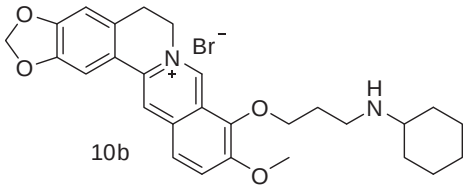

Berberine derivatives with substituted amino groups linked on the 9-position of berberine with different carbon spacers were designed, synthesized, and biologically evaluated as inhibitors of acetylcholinesterase. Compound **10b** with a cyclohexylamino group linked to berberine by a three carbon spacer, gave the most potent inhibitor activity with an IC_{50} value of 0.020 μM for AchE.

Two series of quinoline amide derivatives were prepared and found to be good inhibitors of vascular endothelial growth factor receptor-2 (VEGFR-2). The inhibitory activities were investigated against VEGFR-2 kinase and human umbilical vein endothelial cells (HUVEC) in vitro. Compound **6** (5-chloro-2-hydroxy-*N*-(quinolin-8-yl)benzamide) exhibited the most potent inhibitory activity (IC_{50} = 3.8 and 5.5 nM for VEGFR-2 kinase and HUVEC, respectively). Docking simulation was performed to position compound **6** into the VEGFR-2 ATP-binding site to determine the probable binding model. The results supported the initial pharmacophoric hypothesis and suggested a common mode of interaction at the ATP-binding site of VEGFR-2.

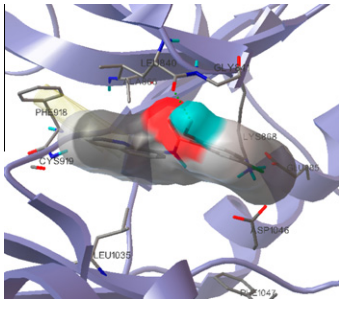

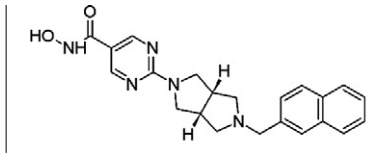

Compound **13** HDAC IC_{50} 13 nM
HCT-116 120 nM
HeLa 260 nM
Orally active in HCT-116 xenograft model

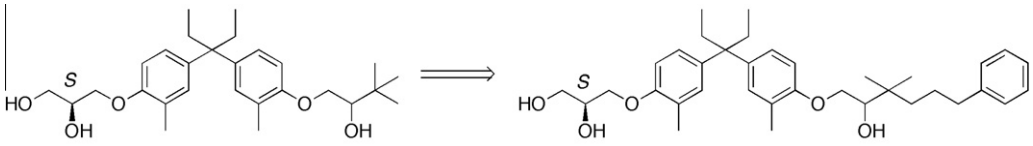

VDR agonist / AR antagonist AR selective antagonist

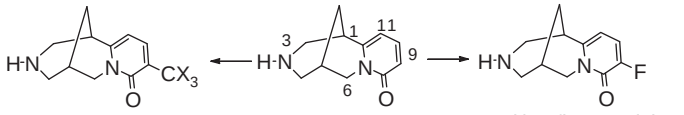

nAChRs *K*i (nM)	X = H	X = F	(-)-cytisine	(-)-9-fluorocytisine
$\alpha_4\beta_2$	0.24	0.22	1.06	6.53
α_7	2000	1000	1000	-

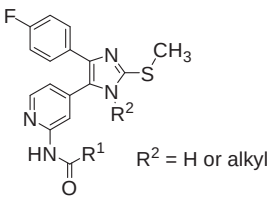

R^2 = H or alkyl

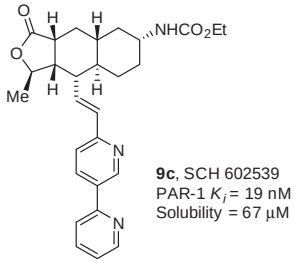

An analog of the thrombin receptor antagonist vorapaxar (SCH 530348) with increased aqueous solubility, compound **9c** (SCH 602539), was discovered through incorporation of polar substituents on the pyridine ring of the himbacine-derived lead series.

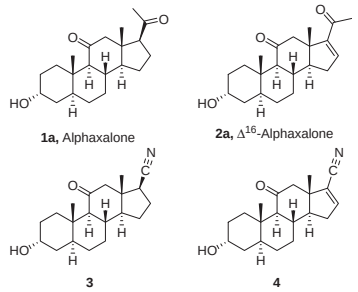

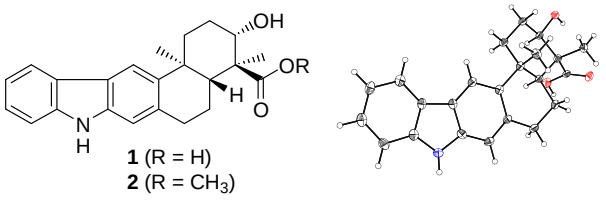

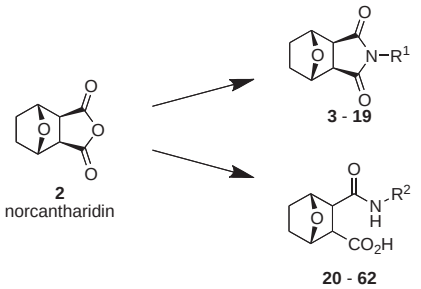

The antiplasmodial activity of 60 norcantharidin analogs is reported.

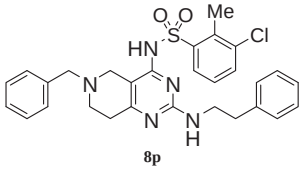

8p
CaMKII Inhibition; IC_{50} = 0.063 μM

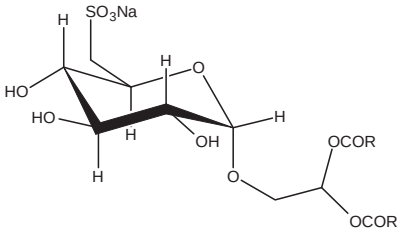

$R = (CH_2)_{14}CH_3$

Phytochemical investigation resulted in isolation of two new lupane-type triterpenoids (**1** and **2**) from the steamed leaves of *Acanthopanax koreanum* (Araliaceae). Compound **1** significantly inhibited LPS-stimulated IL-12, IL-6, and TNF-α production in bone marrow-derived dendritic cells.

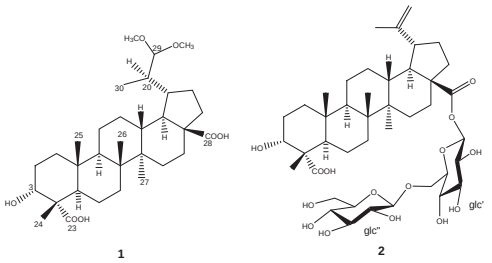

1 **2**

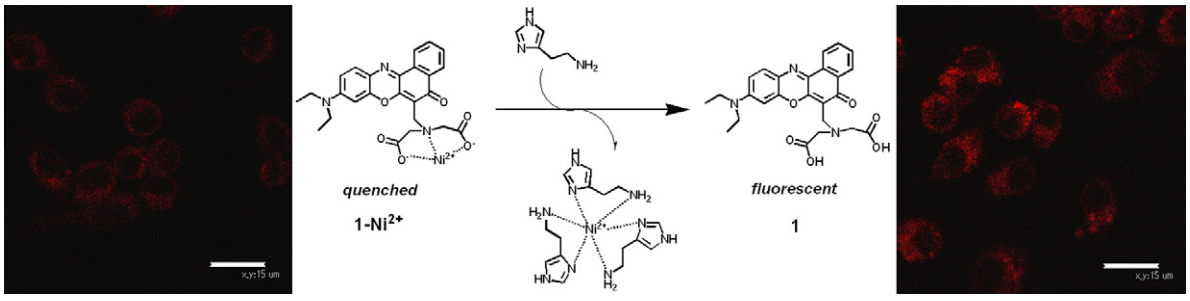

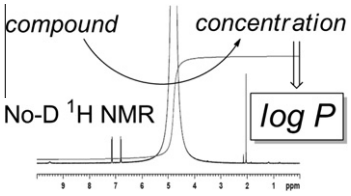

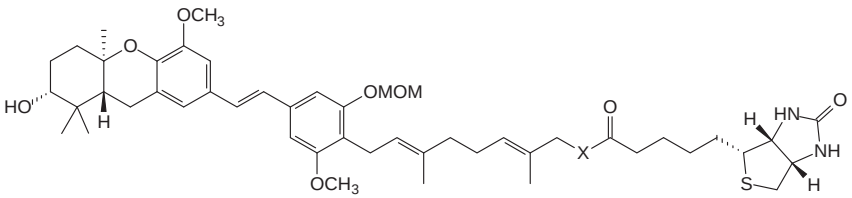

X = O or NH

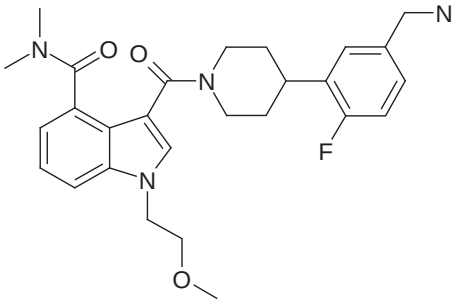

Conformationally constrained β-tryptase inhibitor.

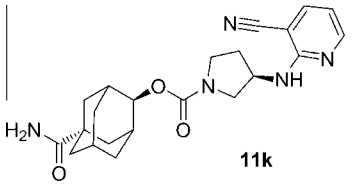

11k

Human 11β-HSD1 enzyme IC_{50} = 0.9 nM

Human 11β-HSD1 adipocyte IC_{50} = 0.4 nM

Rat liver microsome $t_{1/2}$ > 60 min

%F (rat) = 42

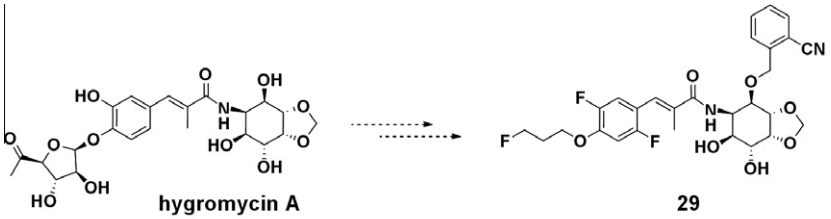

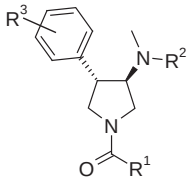

The rational design of a novel series of orally active NK3R antagonists is decribed.

We report a series of potent imidazo[1,2-*a*]pyrazine-based Aurora kinase inhibitors. Optimization of the solvent accessible 8-position led to improvements in both oral bioavailability and off-target kinase inhibition. Compound **25** demonstrates anti-tumor activity in an A2780 ovarian tumor xenograft model.

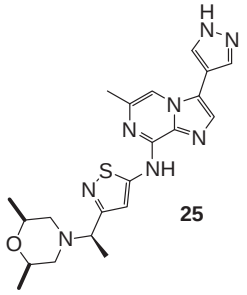

A series of 3-urea-1-(phenylmethyl)-pyridones was discovered as novel EP_3 antagonists via high-throughput screening and subsequent optimization. The synthesis, structure–activity relationships, and optimization of the initial hit that resulted in potent and selective EP_3 receptor antagonists such as **11g** are described.

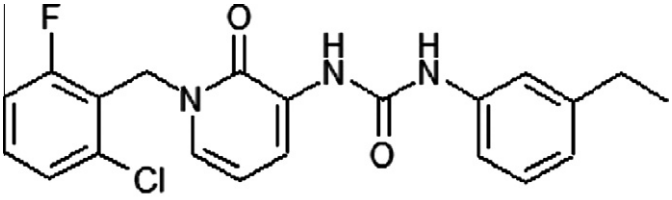

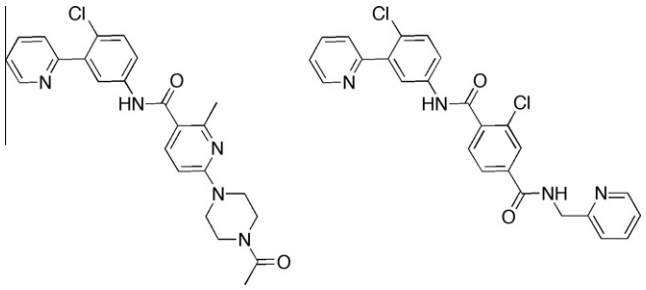

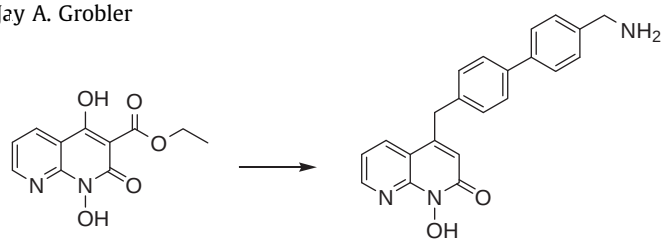

lead compound **1** optimized analog **13**

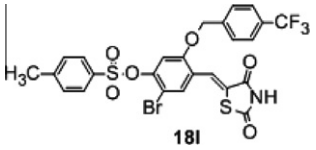

18l

Compound **18l** was a PTP1B inhibitor with IC_{50} of 1.3 μM and activated PPAR-γ at 1.0 μM. It suppressed weight gain in a DIO mouse model system.

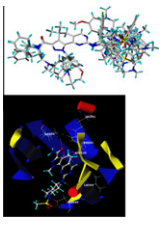

3D-QSAR and docking studies were performed on a series of pyrazolo[4,3-*h*]quinazoline-3-carboxamides as CDK2/CyA inhibitors. The correlation of the results obtained from 3D-QSAR and docking studies can be served as a useful guideline for the further modification of pyrazolo[4,3-*h*]quinazoline-3-carboxamides that function as CDK2/CyA inhibitors.

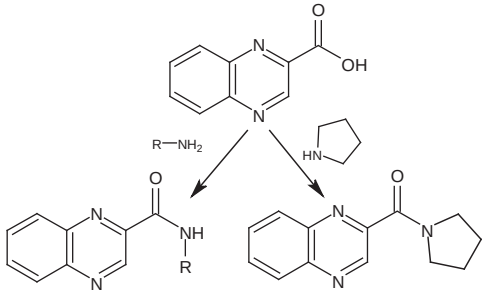

Synthesis, 5-HT$_3$ receptor antagonistic and anti-depressant-like activity of novel quinoxalin-2-carboxamides are described.

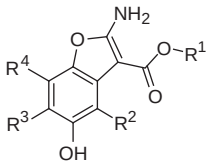

R = alkyl, thio,Cl, ..

Benzofuran-5-ol derivatives were synthesized and tested for in vitro antifungal activity against pathogenic fungi. Among them tested, many of benzofuran-5-ols exhibited potent antifungal activity.

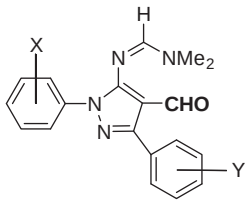

X	Y	GI$_{50}$ (μM) for Antiproliferative activity		
		NCI-H661	NPC-TW01	Jurkat
m-Cl	H	6.9	6.4	8.3
p-Br	H	6.7	7.4	7.3
H	*p*-Me	11.9	9.7	9.5
H	*p*-Cl	8.6	8.1	7.9

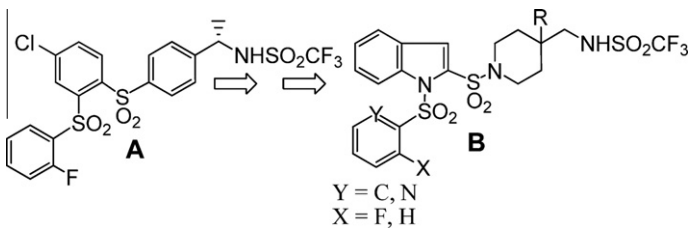

SAR exploration on triaryl bis sulfone **A** led us to structurally novel and diverse CB$_2$ selective ligands **B**.

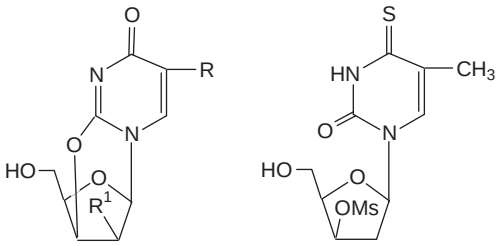

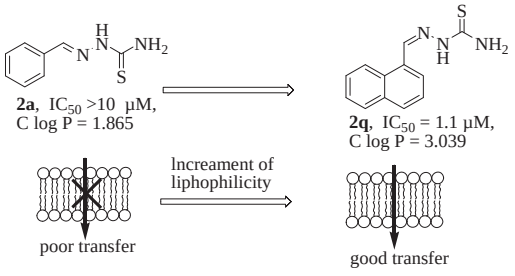

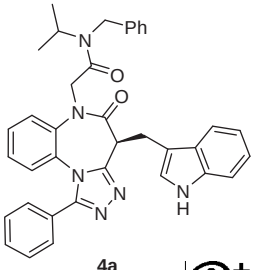

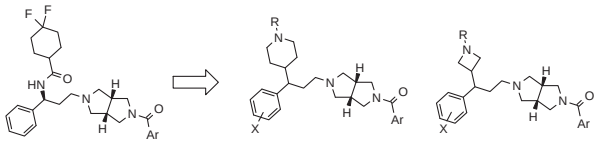

In our CCR5 program, piperidine and azetidine amide replacements as means to improve intrinsic permeability were evaluated. This led to new series of potent CCR5 antagonists, with improved PK behavior.

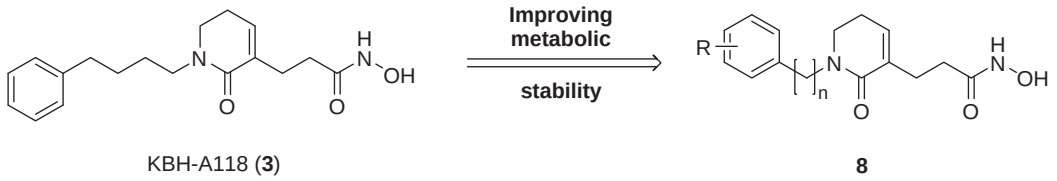

To improve metabolic stability, various analogues were prepared with substituents on aromatic ring of cap group and various chain lengths between the cap group and δ-lactam core.

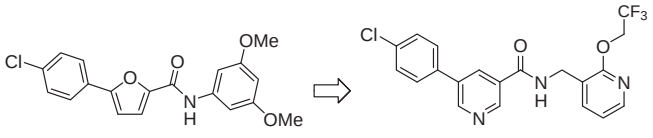

Cancer therapy has moved beyond conventional chemotherapeutics to more mechanism-based targeted approaches. Studies demonstrate that histone deacetylase (HDAC) is a promising target for anticancer agents. Numerous, structurally diverse, hydroxamic acid derivative, HDAC inhibitors have been reported and have been shown to induce growth arrest, differentiation, autophagy, and/or apoptotic cell death by inhibiting multiple signaling pathways in cancer cells. Suberoylanilide hydroxamic acid (SAHA) has emerged as an effective anticancer therapeutic agent and was recently approved by FDA for the treatment of advanced cutaneous T-cell lymphoma. In our previous study, we reported the development of the novel selenium-containing potent HDAC inhibitors, SelSA-1 and SelSA-2. In this study, the effects of SelSA-1 and SelSA-2 on signaling pathways and cytotoxicity were compared with the known HDAC inhibitor, SAHA, in lung cancer cell lines. After 24 h of treatment, SelSA-1 and SelSA-2 inhibited lung cancer cell growth to a greater extent than SAHA in a dose-dependent manner with IC_{50} values at low micromolar concentrations. SelSA-1 and SelSA-2 inhibited ERK and PI3K-AKT signaling pathways while simultaneously increasing in autophagy in A549 cells in a time dependent manner. This preliminary study demonstrates the effectiveness of the selenium-containing analogs of SAHA, SelSA-1, and SelSA-2, as HDAC inhibitors and provides insight into the improvement and/or development of these analogs as a therapeutic approach for the treatment of lung cancer.

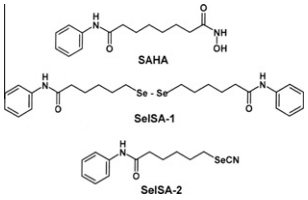

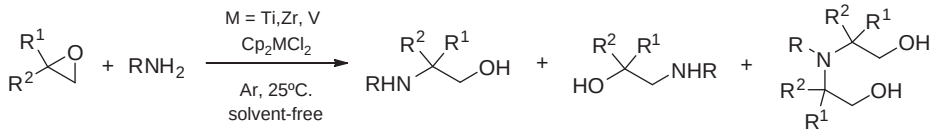

Metallocenes have been evaluated as catalyst in the solvent free, room temperature, preparation of fungistatic vicinal aminoalcohols. The fungistatic activity of the prepared compounds against *Botrytis cinerea* and *Colletotrichum gloeosporioides* is discussed.

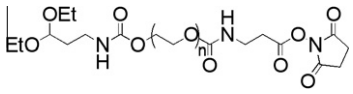

The development of polymeric formulations as drug carriers often requires incorporation of heterobifunctional PEGs capable of sequentially reacting with targeting ligands and structural components of nanoparticles/liposomes. This paper describes efficient syntheses of heterobifunctional PEGs and associated conjugation methodologies.

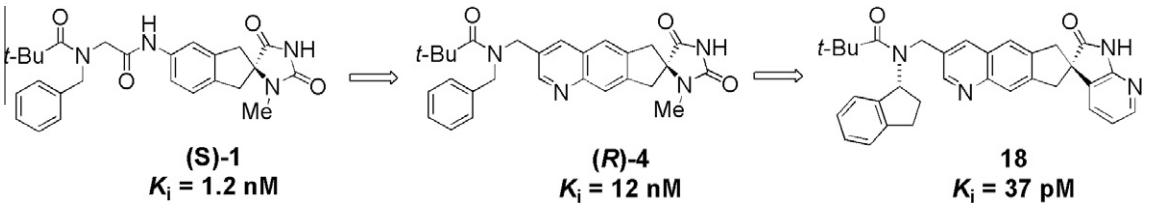

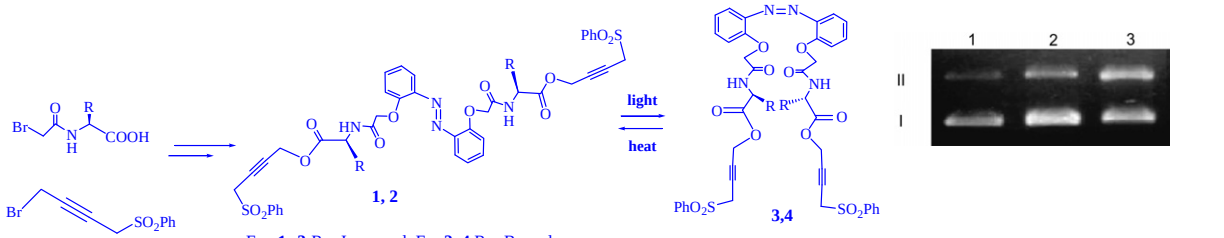

For **1**, **3** R = Isopropyl, For **2**, **4** R = Benzyl

3,**4** are better DNA cleaving agents than **1**, **2** under basic pH

Lane 1: DNA, Lane 2: DNA + Sulfone 2
Lane 3: DNA + Sulfones 4+2(1.5:1)

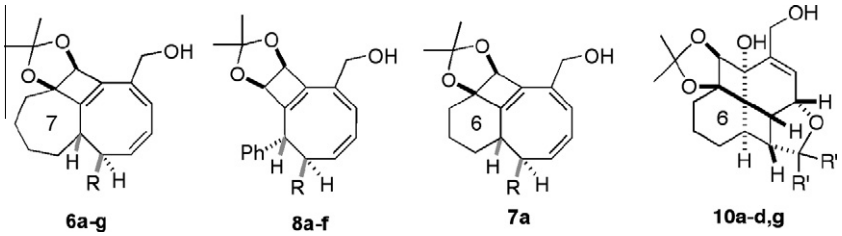

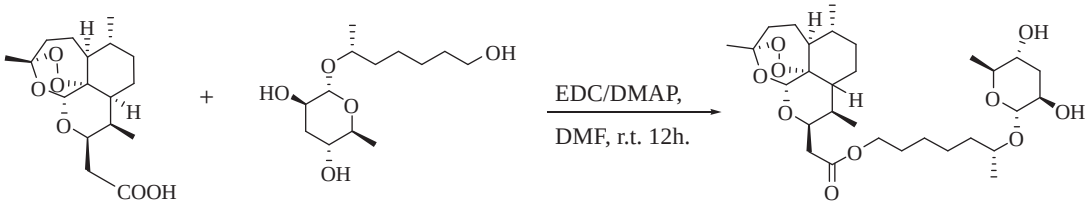

Novel hybrids of artemisinin–glycolipid were synthesized. Some of these hybrids showed potent in vivo antiangiogenic activity that was higher than or comparable to those of fumagillin and thalidomide at a concentration of 2.5 nmol.

OTHER CONTENTS

*Corresponding author
Supplementary data available via ScienceDirect

COVER

Overlay of high resolution co-crystal structures of *R*-**22**-ADP (cyan) and **1**-ADP (green) bound in an allosteric binding site of the mitotic kinesin KSP. [Roecker, A. J.; Coleman, P. J.; Mercer, S. P.; Schreier, J. D.; Buser, C. A.; Walsh, E. S.; Hamilton, K.; Lobell, R. B.; Tao, W.; Diehl, R. E.; South, V. J.; Davide, J. P.; Kohl, N. E.; Yan, Y.; Kuo, L. C.; Li, C.; Fernandez-Metzler, C.; Mahan, E. A.; Prueksaritanont, T.; Hartman, G. D. *Bioorg. Med. Chem. Lett.* **2007**, *17*, 5677.]

Indexed/Abstracted in: Beilstein, Biochemistry & Biophysics Citation Index, CANCERLIT, Chemical Abstracts, Chemistry Citation Index, Current Awareness in Biological Sciences/BIOBASE, Current Contents: Life Sciences, EMBASE/Excerpta Medica, MEDLINE, PASCAL, Research Alert, Science Citation Index, SciSearch, TOXFILE. Also covered in the abstract and citation database SCOPUS®. Full text available on ScienceDirect®

ELSEVIER

ISSN 0960-894X